Hexylthiophene-Functionalized Carbazole Dyes for Efficient Molecular Photovoltaics: Tuning of Solar-Cell Performance by Structural Modification

Zhong-Sheng Wang,*,† Nagatoshi Koumura,*,† Yan Cui,† Masabumi Takahashi,‡ Hiroki Sekiguchi,‡ Atsunori Mori,‡ Toshitaka Kubo,† Akihiro Furube,† and Kohjiro Hara*,†

National Institute of Advanced Industrial Science and Technology, 1-1-1 Higashi, Tsukuba, Ibaraki 305-8565, Japan, and Department of Chemical Science and Engineering, Kobe University, 1-1 Rokkodai, Noda-ku, Kobe, Hyogo 657-8501, Japan

Received February 1, 2008. Revised Manuscript Received March 24, 2008

Novel organic dyes (**MK** dyes), which have a carbazole derivative as an electron donor and a cyanoacrylic acid moiety (═C(—C≡N)COOH) as an electron acceptor and an anchoring group, connected with *n*-hexyl-substituted oligothiophenes as a π-conjugated system, were designed and synthesized for application in dye-sensitized solar cells (DSSCs), which are one of the promising molecular photovoltaics. The photovoltaic performance of the DSSCs based on **MK** dyes markedly depends on the molecular structure of the dyes in terms of the number and position of *n*-hexyl chains and the number of thiophene moieties. Retardation of charge recombination caused by the existence of *n*-hexyl chains linked to the thiophene groups resulted in an increase in electron lifetime. As a consequence, an improvement of open-circuit photovoltage (V_{oc}) and hence the solar-to-electric power conversion efficiency (η) of DSSCs was achieved upon addition of *n*-hexyl chains to the thiophene groups. In addition, the adsorption condition (amount of dye molecules and/or dye aggregate thickness) on the nanoporous TiO_2 electrode, depending on the number of hexyl chains, strongly affected the performance of DSSCs. A larger amount and/or thicker aggregate of dye molecules brought about longer electron lifetime, which resulted in higher V_{oc}, and slower diffusion of I_3^- ions in the nanoporous TiO_2 electrode, which led to lower short-circuit photocurrent (J_{sc}) and fill factor (FF). In the result of thorough investigation on the series of **MK** dyes, a DSSC based on **MK-2** consisting of *n*-hexyl-substituted quarter-thiophene produced 8.3% of η (J_{sc} = 15.22 mA cm^{-2}, V_{oc} = 0.73 V, and FF = 0.75) under 100 mW cm^{-2} simulated AM1.5G solar irradiation.

Introduction

Dye-sensitized solar cells (DSSCs), which are one of the promising molecular photovoltaics, have been attracting considerable attention since the pioneering study[1] because of the potential of low-cost production and high efficiency. In order to improve the solar-to-electric power conversion efficiency (η), both metal complexes[2–8] and metal-free organic dyes,[9–15] as sensitizers of nanocrystalline TiO_2 electrode, have been extensively investigated and developed in terms of optical absorption extension to the red or infrared region through molecular design. The highest η for DSSCs has so far reached 11% obtained from Ru polypyridine complexes.[16,17] In addition, DSSCs based on Ru complexes with ionic liquid[18] or gelated[19] redox electrolyte exhibited good long-term stability under light soaking at 60 °C or under dark at 80 °C.

Recently, many scientists are paying a good deal of attention to organic dyes for use in DSSCs due to their high extinction coefficient, facile molecular design, and no

* To whom correspondence should be addressed. Tel.: +81-29-861-4638. Fax: +81-29-861-4638. E-mail: zs.wang@aist.go.jp (Z.-S.W.), n-koumura@aist.go.jp (N.K.), and k-hara@aist.go.jp (K.H.).
† National Institute of Advanced Industrial Science and Technology.
‡ Kobe University.

(1) O'Regan, B.; Grätzel, M. *Nature* **1991**, *353*, 737.
(2) Nazeerudin, M. K.; Kay, A.; Rodicio, I.; Humphry-Baker, R.; Müller, E.; Liska, P.; Vlachopoulos, N.; Grätzel, M. *J. Am. Chem. Soc.* **1993**, *115*, 6382.
(3) Nazeeruddin, M. K.; Péchy, P.; Renouard, T.; Zakeeruddin, S. M.; Humphry-Baker, R.; Comte, P.; Liska, P.; Cevey, L.; Costa, E.; Shklover, V.; Spiccia, L.; Deacon, G. B.; Bignozzi, C. A.; Grätzel, M. *J. Am. Chem. Soc.* **2001**, *123*, 1613.
(4) Wang, Z.-S.; Huang, C.-H.; Zhang, B.-W.; Hou, Y.-J.; Xie, P.-H.; Qian, H.-J.; Ibrahim, K. *New J. Chem.* **2000**, *24*, 567.
(5) Kukrek, A.; Wang, D.; Hou, Y.; Zong, R.; Thummel, R. *Inorg. Chem.* **2006**, *45*, 10131.
(6) Wang, Z.-S.; Huang, C.-H.; Huang, Y.-Y.; Zhang, B.-W.; Xie, P.-H.; Hou, Y.-J.; Ibrahim, K.; Qian, H.-J.; Liu, F.-Q. *Sol. Energy Mater. Sol. Cells* **2002**, *71*, 261.
(7) Islam, A.; Chowdhury, F. A.; Chiba, Y.; Komiya, R.; Fuke, N.; Ikeda, N.; Nozaki, K.; Han, L. *Chem. Mater.* **2006**, *18*, 5178.
(8) Hoertz, P. G.; Carlisle, R. A.; Meyer, G. J.; Wang, D.; Piotrowiak, P.; Galoppini, E. *Nano Lett.* **2003**, *3*, 325.
(9) Kim, S.; Lee, J. K.; Kang, S. O.; Ko, J.; Yum, J.-H.; Fantacci, S.; De Angelis, F.; Di Censo, D.; Nazeeruddin, Md. K.; Grätzel, M. *J. Am. Chem. Soc.* **2006**, *128*, 16701.
(10) Horiuchi, T.; Miura, H.; Sumioka, K.; Uchida, S. *J. Am. Chem. Soc.* **2004**, *126*, 12218.
(11) Wang, Z.-S.; Li, F.-Y.; Huang, C.-H.; Wang, L.; Wei, M.; Jin, L.-P.; Li, N.-Q. *J. Phys. Chem. B* **2000**, *104*, 9676.
(12) Kitamura, T.; Ikeda, M.; Shigaki, K.; Inoue, T.; Anderson, N. A.; Ai, X.; Lian, T.; Yanagida, S. *Chem. Mater.* **2004**, *16*, 1806.
(13) Hara, K.; Sato, T.; Katoh, R.; Furube, A.; Ohga, Y.; Shinpo, A.; Suga, S.; Sayama, K.; Sugihara, H.; Arakawa, H. *J. Phys. Chem. B* **2003**, *107*, 597.
(14) Velusamy, M.; Justion Thomas, K. R.; Lin, J. T.; Hsu, Y.-C.; Ho, K.-C. *Org. Lett.* **2005**, *7*, 1899.
(15) Qin, P.; Yang, X.; Chen, R.; Sun, L.; Marinado, T.; Edvinsson, T.; Boschloo, G.; Hagfeldt, A. *J. Phys. Chem. C* **2007**, *111*, 1853.

10.1021/cm8003276 CCC: $40.75 © 2008 American Chemical Society
Published on Web 05/29/2008

concern with the noble metal resource. In the past, various kinds of metal-free organic dyes[9–15,20–29] have been developed as sensitizers in DSSCs, and the η has been improved gradually through molecular design. Among them, coumarin dyes are promising due to the high efficiency and good stability.[30] We have systematically studied coumarin dyes as sensitizers in DSSCs in the past several years. The η of a DSSC based on NKX-2677 bearing a bithiophene and a cyanoacrylic acid moiety reached 7.4%.[31] After that, a DSSC with NKX-2700 having one methine group inserted between the two thiophenes, whose maximum absorption is red-shifted as compared to NKX-2677, produced 8.2% of η,[32] which was close to the efficiency obtained from a DSSC based on *cis*-di(thiocyanato)-bis(2,2′-bipyridyl-4,4′-dicarboxylate) ruthenium(II) (N719 dye) under a comparable condition.

However, the performances of DSSCs based on organic dyes have not yet exceeded the performances of those based on Ru complexes. For example, high content of deoxycholic acid (DCA) as a coadsorbate in the dye solution and high molar amount (e.g., 1.0 M) of 4-*tert*-butylpyridine (TBP) in the redox electrolyte as an additive are required to obtain high η values for DSSCs based on coumarin dyes.[33] DCA was used to abate the strong intermolecular interaction and thus break up dye aggregation; the latter would reduce solar-cell performance. The aim of using TBP was to suppress charge recombination and to raise the conduction band edge so as to acquire higher open-circuit photovoltage (V_{oc}) of DSSCs.[34,35] The V_{oc} for a DSSC depends, in principle, on the conduction band edge of TiO_2, E_{CB}, and the redox potential of the redox couple. However, charge recombination processes of injected electrons with dye cations (CR1) and with I_3^- ions in the electrolyte (CR2) make the actual V_{oc} lower than the theoretic value.[36] Despite the aid of DCA and TBP, the V_{oc} for the DSSCs based on coumarin dyes is still lower than that of DSSCs with Ru complexes due to the serious charge recombination.[31,32] The previous results imply that serious charge recombination for coumarin dye based DSSCs result from the strong intermolecular $\pi-\pi$ interaction of dye molecules. Therefore, new dye molecules with weak intermolecular $\pi-\pi$ interaction should be designed for high V_{oc} and hence high η in organic dye based DSSCs.

In general, the molecular structure of an organic dye for DSSCs has been designed and synthesized based on several basic concepts that are the following: (1) matching of oxidation potentials of the ground and exited states for a dye, which are usually replaced by the highest occupied molecular orbital (HOMO) and the lowest unoccupied molecular orbital (LUMO), with the energy levels of I^-/I_3^- redox potential and E_{CB} of the TiO_2 electrode, respectively; (2) a donor-π-conjugation-linkage-acceptor (D-Π-A) structure required for a wide range absorption extending to the near-infrared or infrared region; and (3) one or two anchoring groups such as carboxylic acid[2] or sulfonic acid[37] groups required for a strong adsorption onto the surface of TiO_2. According to the previous reports of organic dyes used in DSSCs so far, the combination of a *para*-bisubstituted aniline (donor) with a cyanoacrylic acid (acceptor and anchor), such as coumarin dyes,[31,32] brings about good matching of the above-mentioned energy levels. In these cases, an oligothiophene moiety was successfully selected as the conjugation unit of the dye molecule between the donor and acceptor groups, resulting in maximum absorption bands shifting to the longer wavelength.[31] However, the strong intermolecular $\pi-\pi$ interaction with increasing thiophene number leads to dye aggregation, which was usually prevented by coadsorption of DCA[31–33] as we mentioned above.

According to the above-mentioned points, we have designed and synthesized a new series of dye molecules based on a carbazole moiety as a donor, alkyl-functionalized oligothiophenes as a π-conjugation linkage, and a cyanoacrylic acid as an acceptor and anchoring group, shown in Figure 1. It is well-known that carbazole derivatives (for example, 3-amino-9-ethylcarbazole) are commercially available, so that the synthetic scheme of dye molecules can be simplified. We can add several functions to these dyes by the structural modification on the thiophene rings. With a long alkyl chain substituted to the thiophene ring, an increase in electron lifetime (τ) can be expected by preventing the approach of acceptors (i.e., I_3^- ions) to the TiO_2 surface and/

(16) Chiba, Y.; Islam, A.; Watanabe, Y.; Komiya, R.; Koide, N.; Han, L. *Jpn. J. Appl. Phys.* **2006**, *45*, L638.
(17) Nazeeruddin, M. K.; Angelis, F. D.; Fantacci, S.; Selloni, A.; Viscardi, G.; Liska, P.; Ito, S.; Takeru, B.; Grätzel, M. *J. Am. Chem. Soc.* **2005**, *127*, 16835.
(18) Kuang, D.; Wang, P.; Ito, S.; Zakeeruddin, S. M.; Grätzel, M. *J. Am. Chem. Soc.* **2006**, *128*, 7732.
(19) Wang, P.; Zakeeruddin, S. M.; Moser, J. E.; Nazeeruddin, M. K.; Sekiguchi, T.; Grätzel, M. *Nat. Mater.* **2003**, *2*, 402.
(20) (a) Liang, M.; Xu, W.; Cai, F.; Chen, P.; Peng, B.; Chen, J.; Li, Z. *J. Phys. Chem. C* **2007**, *111*, 4465. (b) Hwang, S.; Lee, J.-H.; Park, C.; Lee, H.; Kim, C.; Park, C.; Lee, M.-H.; Lee, W.; Park, J.; Kim, K.; Park, N.-G.; Kim, C. *Chem. Commun.* **2007**, 4887.
(21) Zhang, X.-H.; Li, C.; Wang, W.-B.; Cheng, X.-X.; Wang, X.-S.; Zhang, B.-W. *J. Mater. Chem.* **2007**, *17*, 642.
(22) Hara, K.; Sato, T.; Katoh, R.; Furube, A.; Yoshihara, T.; Murai, M.; Kurashige, M.; Ito, S.; Shinpo, A.; Suga, S.; Arakawa, H. *Adv. Funct. Mater.* **2005**, *15*, 246.
(23) Wang, Z.-S.; Li, F.-Y.; Huang, C.-H. *Chem. Commun.* **2000**, 2063.
(24) He, J.; Benko, G.; Korodi, F.; Polivka, T.; Lomoth, R.; Akermark, B.; Sun, L.; Hagfeldt, A.; Sundström, V. *J. Am. Chem. Soc.* **2002**, *124*, 4922.
(25) Kroeze, J. E.; Savenije, T. J.; Warman, J. M. *J. Am. Chem. Soc.* **2004**, *126*, 7608.
(26) Wang, Z.-S.; Sayama, K.; Sugihara, H. *J. Phys. Chem. B* **2005**, *109*, 22449.
(27) Wang, Z.-S.; Huang, C.-H.; Li, F.-Y.; Weng, S.-F.; Ibrahim, K.; Liu, F.-Q. *J. Phys. Chem. B* **2001**, *105*, 4230.
(28) Otaka, H.; Kira, M.; Yano, K.; Ito, S.; Mitekura, H.; Kawata, T.; Matsui, F. *J. Photochem. Photobiol., A* **2004**, *164*, 67.
(29) Li, S.-L.; Jiang, K.-J.; Shao, K.-F.; Yang, L.-M. *Chem. Commun.* **2006**, 2792.
(30) Wang, Z.-S.; Cui, Y.; Dan-oh, Y.; Kasada, C.; Shinpo, A.; Hara, K. *Adv. Mater.* **2007**, *19*, 1138.
(31) Hara, K.; Wang, Z.-S.; Sato, T.; Furube, A.; Katoh, R.; Sugihara, H.; Dan-oh, Y.; Kasada, C.; Shinpo, A.; Suga, S. *J. Phys. Chem. B* **2005**, *109*, 15476.
(32) Wang, Z.-S.; Cui, Y.; Dan-oh, Y.; Kasada, C.; Shinpo, A.; Hara, K. *J. Phys. Chem. C* **2007**, *111*, 7224.
(33) Hara, K.; Dan-oh, Y.; Kasada, C.; Ohga, Y.; Shinpo, A.; Suga, S.; Sayama, K.; Arakawa, H. *Langmuir* **2004**, *20*, 4205.
(34) Huang, S. Y.; Schlichthörl, G.; Nozik, A. J.; Grätzel, M.; Frank, A. J. *J. Phys. Chem. B* **1997**, *101*, 2576.
(35) Boschloo, G.; Häggman, L.; Hagfeldt, A. *J. Phys. Chem. B* **2006**, *110*, 13144.
(36) Hagfeldt, A.; Grätzel, M. *Chem. Rev.* **1995**, *95*, 49.
(37) Wang, Z.-S.; Li, F.-Y.; Huang, C.-H. *J. Phys. Chem. B* **2001**, *105*, 9210.

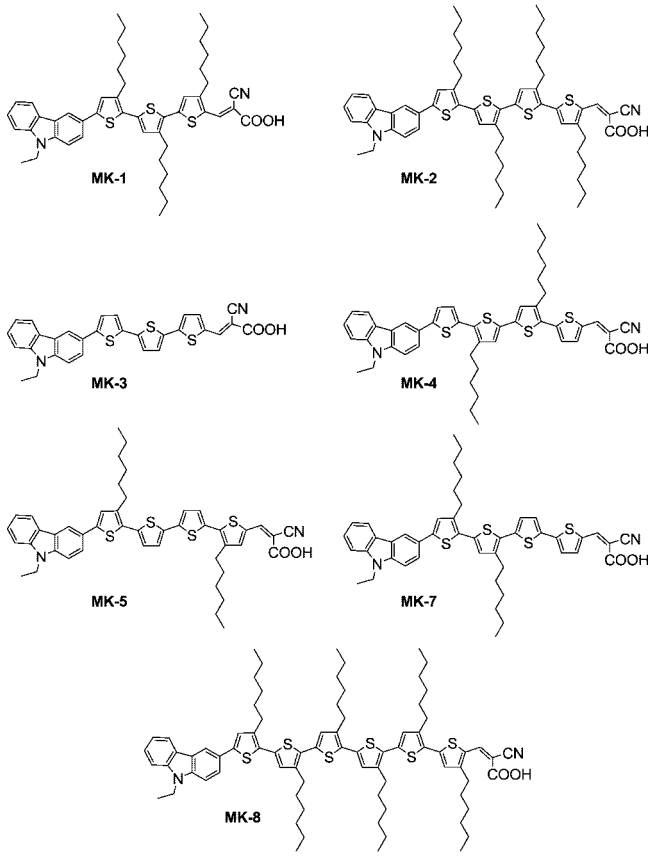

Figure 1. Molecular structures of **MK** dyes.

or by reducing the reorganization energy of the dye. Most recently, we proposed the concept of this molecular design in our previous communication where alkyl chains linked to the oligothiophene moiety were effective to suppress charge recombination and hence to improve V_{oc}.[38]

In this article, we designed and synthesized a series of **MK** dyes, which have various hexyl-substituted oligothiophene moieties as a π-conjugated system, and systematically studied the effect of molecular structures of **MK** dyes, especially the thiophene number and alkyl chain number and position, on the photophysical, photochemical, and electrochemical properties of dyes, solar-cell performance, and the kinetics for electron injection and charge recombination. Our results strongly indicate that interfacial engineering by means of molecular design is important for highly efficient solar-cell performance of DSSCs.

Experimental Section

Syntheses of MK Dyes. The detailed procedures for the syntheses of dye molecules is described in Supporting Information based on several references[39,40] for the synthetic technique of oligothiophenes.

Materials and Reagents. Regent-grade LiI, I_2, $LiClO_4$, $TiCl_4$, acetonitrile (AN), tetrahydrofuran (THF), chloroform (Wako Pure Chemical Industries Ltd.), 3-methoxypropionitrile (MPN, Tokyo Chemical Industry Co., Ltd.), and toluene (Kanto Chemical Co., Inc.) were used without further purification. 1,2-Dimethyl-3-*n*-propylimidazolium iodide (DMPImI) and TBP were purchased from Tomiyama Pure Chemical Industries Ltd. Transparent conducting oxide (TCO, F-doped SnO_2, 10 Ω/□, Nippon Sheet Glass Co.) was washed with a basic solution, ethanol, and acetone successively under supersonication for 10 min each before use.

Characterization. The UV−vis absorption spectra of the dye-loaded transparent film and the dye solutions were recorded on a Shimadzu UV-3101PC spectrophotometer. Fourier transform infrared (FT-IR) spectra were measured with a Perkin-Elmer Spectrum One spectrophotometer with an attenuated total reflection (ATR) system equipped with a ZnSe prism. Cyclic voltammetry (CV) was measured with a three-electrode electrochemical cell on a CHI610B electrochemical analyzer. Dye-loaded film, platinum, and Ag/Ag^+ (0.01 M $AgNO_3$ + 0.1 M tetrabutylammonium perchlorate in AN) were employed as working, counter, and reference electrodes, respectively. The supporting electrolyte was 0.1 M $LiClO_4$ in AN, which was degassed with N_2 for 20 min prior to scanning. The potential of the reference electrode is 0.49 V versus NHE, and it was calibrated with ferrocene immediately after CV measurement. Electrochemical impedance spectroscopy (EIS) for DSSCs under AM1.5G light were measured with an impedance/gain-phase analyzer (Solartron SI 1260) connected with a potentiostat (Solartron SI 1286). The spectra were scanned in a frequency range of $0.1-10^5$ Hz at room temperature with applied potential set at open-circuit. The alternate current (AC) amplitude was set at 10 mV.

NC-AFM Measurement. Noncontact atomic force microscopy (NC-AFM) measurements were performed in an ultrahigh vacuum scanning probe microscopy (UHV-SPM) chamber (JEOL model JAFM-4400) with a base pressure of $<1.4 \times 10^{-8}$ Pa. Cone-shaped silicon cantilevers with $f_0 = 140-290$ kHz and $k = 4-14$ N/m (Silicon-MDT Ltd.), which were highly doped with B (0.002 Ω cm) and coated with W_2C (25 nm thick, 30 $\mu\Omega$ cm), were used. All measurements were performed at room temperature by the constant frequency shift condition. The rutile TiO_2 (110) single crystal substrate (Nakazumi Crystal) was used for NC-AFM measurements. The sample surface was cleaned by several cycles of Ar^+-ion sputtering (2 keV) and annealed in the UHV-SPM chamber. Vacuum pressure during annealing did not exceed 5×10^{-7} Pa. Typical heating and cooling rates were several °C/s. Temperature was measured with an optical pyrometer. After the substrates were prepared in UHV, they were immersed in a toluene solution of the **MK-2** (0.3 mM) for 20 min at room temperature. The dye adsorbed substrate was copiously rinsed respectively with toluene and AN followed by drying with N_2.

Transient Absorption Spectroscopy. The light source for the femtosecond pump−probe transient absorption measurements was a regenerative amplifier system of a Ti:sapphire laser (800 nm wavelength, 160 fs fwhm pulse width, 1.0 mJ/pulse intensity, 1 kHz repetition, Spectra Physics, Hurricane) combined with two optical parametric amplifiers (OPAs; Quantronix, Topas). For a pump pulse, the output of the OPA at a wavelength of 540 nm with an intensity of several μJ per pulse at a 500-Hz modulation frequency was used, and for a probe pulse, the output of the other OPA at 3440 nm was used. The probe beam was focused on the center of the pump beam on the sample and then detected with an MCT photodetector (Hamamatsu, P3257-10) after passing through an interference filter to remove undesired light. The instrumental time response was about 200 fs, as determined from the rise time of transient absorption of a thin silicon plate. All measurements were carried out at 295 K.

Fabrication of Dye-Sensitized TiO_2 Photoelectrode. Paste **N**, comprising nanoparticles (~20 nm), and paste **M**, comprising 70%

(38) Koumura, N.; Wang, Z.-S.; Mori, S.; Miyashita, M.; Suzuki, E.; Hara, K. *J. Am. Chem. Soc.* **2006**, *128*, 14256.
(39) Takahashi, M.; Masui, K.; Sekiguchi, H.; Kobayashi, N.; Mori, A.; Funahashi, A.; Tamaoki, N. *J. Am. Chem. Soc.* **2006**, *128*, 10930.
(40) Masui, K.; Ikegami, H.; Mori, A. *J. Am. Chem. Soc.* **2004**, *126*, 5074.

Table 1. Absorption and Electrochemical Properties of MK Dyes and Adsorbed Dye Amount on TiO_2 Films[a]

dye	λ_{max}, nm (ε, M^{-1} cm^{-1})	λ_{max}, nm (on TiO_2)	$\Gamma/10^{-8}$ (mol cm^{-2} μm^{-1})	HOMO (V vs NHE)	gap (eV)	LUMO (V vs NHE)
MK-1	480 (38800)	427	1.7	1.07	1.90	−0.83
MK-2	480 (38400)	441	1.9	0.96	1.85	−0.89
MK-3	485 (40100)	402	5.4	0.99	1.77	−0.78
MK-4	474 (33100)	414	6.5	0.86	1.71	−0.85
MK-5	473 (38600)	424	6.2	0.83	1.70	−0.87
MK-7	478 (39300)	416	3.2	0.98	1.72	−0.74
MK-8	471 (46900)	455	2.2	1.09	1.70	−0.61

[a] λ_{max} and the corresponding ε were obtained from the dye solutions in a mixture solvent of THF/toluene by a volume ratio of 2/8. The formal oxidation potential of the dye-loaded TiO_2 film is taken as the HOMO, and the LUMO is calculated with the expression of LUMO = HOMO − gap, where the gap is derived from the absorption onset wavelength of the dye-loaded film. Γ is the surface concentration of the dye on the TiO_2 film.

nanoparticles (~20 nm) and 30% large particles (~100 nm), were prepared using ethyl cellulose as a binder and α-terpineol as a solvent.[41] Transparent TiO_2 films (3.9 ± 0.1 μm thick, 5 mm × 5 mm in size) were fabricated by screen-printing paste **N** one time while double layer TiO_2 films (~16 μm) were fabricated by screen-printing paste **N** three times and then paste **M** one time on the TCO glass, followed by calcinations at 525 °C for 2 h. The film thickness was measured with a Tencor Alpha-Step 500 Surface Profiler. The sintered TiO_2 films were impregnated in a 0.05 M $TiCl_4$ aqueous solution at 70 °C for 30 min using the reported method[3] and then washed with distilled water followed by drying with a nitrogen flow. The $TiCl_4$-treated TiO_2 films were then heated at 450 °C for 30 min. After the TiO_2 film was taken from the furnace while it was still hot (~ 100 °C), it was dipped in 0.3 mM dye solution in toluene overnight. Then, the dye-loaded TiO_2 film was withdrawn from the dye solution and washed copiously with toluene and AN, respectively, followed by drying with a nitrogen stream before solar cell fabrication. The dye-loaded TiO_2 film as working electrode and the Pt-coated TCO as counter electrode were separated by a hot-melt Surlyn film (30 μm) and sealed together by pressing them under heat (105 °C). The electrolyte was introduced into the interspace between the working and the counter electrodes from the two holes predrilled on the back of the counter electrode. Then, the two holes were sealed with a Surlyn film covered with a thin glass slide under heat (105 °C). This work employs three kinds of redox electrolytes: **A**, 0.6 M DMPImI + 0.1 M LiI + 0.05 M I_2 + 0.5 M TBP in MPN; **B**, replacing MPN in electrolyte **A** with AN; and **C**, 0.2 M instead of 0.05 M I_2 in electrolyte **B**.

Photovoltaic Measurement. Photocurrent action spectra were recorded on a CEP-99W system (Bunkoh-Keiki Co., Ltd.) by illuminating DSSCs with direct current (DC) mode and high-intensity monochromatic light (e.g., 5 mW cm^{-2}) without bias white light. The current−voltage characteristics of sealed DSSCs were measured on a computer-controlled current−voltage source meter (Advantest, R6243) under illumination of simulated AM1.5G solar light from an AM1.5 solar simulator (Wacom Co., Japan, WXS-80C-3 with a 300-W Xe lamp and an AM1.5 filter). The incident light intensity was calibrated by using a standard crystalline silicon solar cell, which was produced and calibrated by Japan Quality Assurance Organization, with an IR-cutoff filter (Schott, KG-5), giving the photoresponse range of amorphous silicon solar cell. To avoid the diffuse light penetrating into the active dye-loaded film, a black mask with an aperture area of 0.2354 cm^2, measured with an optical microscope, LEICA M420, equipped with a digital camera (Nikon DXM1200), was employed to test photovoltaic performance. We did not calculate the mismatch factor for calibration of current and efficiency. However, considering that the J_{sc} of DSSCs in this work at 100 mW cm^{-2} simulated AM1.5G light is ~5% smaller than the integrated current density from IPCE spectrum and AM1.5G solar emission spectrum, suggesting the η measured in this work is not overestimated.

Results and Discussion

Absorption and Electrochemical Properties of MK Dyes. The UV−vis absorption properties in a mixture solvent of THF/toluene (volume ratio of 2/8) and electrochemical properties of **MK** dyes are shown in Table 1. Owing to their similar structure, all the **MK** dyes studied in this work exhibit similar $\pi-\pi^*$ electron transition peaks located in the range of 470−485 nm. The values of molar extinction coefficient, ε, at the maximum absorption wavelength, λ_{max}, for these dyes are in the range of $3.31 - 4.69 \times 10^4$ dm^3 mol^{-1} cm^{-1}. A bathochromic effect of the $\pi-\pi^*$ transition peak for the **MK** dyes was observed with increasing the polarity of solvent,[42] for example, from toluene to chloroform.

The **MK** dye molecules are able to bond to the TiO_2 surface through carboxylate group, as evidenced by attenuated total reflection FT-IR data (Supporting Information), where the characteristic IR peak for −C═O in the −COOH group (1676 cm^{-1}) in neat dye disappeared but, instead, two new IR peaks for the $-COO^-$ group (1590 and 1387 cm^{-1}) were observed for the dye-loaded TiO_2 film.[43] Normalized UV−vis absorption spectra of the **MK** dyes adsorbed on thin TiO_2 films are shown in Figure 2, and the λ_{max} for the dye-loaded TiO_2 film is also listed in Table 1. Compared to the absorption properties in solution (Table 1), all the **MK** dyes show blue shifts of λ_{max}, attributable to the solvent effect[42] and the deprotonation,[3,44] upon dye adsorption on the TiO_2 surface, of the carboxylic acid present in the dye.

It is clearly seen from Figure 2a that the maximum absorption peak gradually shifts to the longer wavelength with increasing the number of the thiophene group as a result of expanded π-conjugation. For the dyes with fixed number of thiophenes, the number and position of hexyl chains influenced the absorption spectrum. Less hexyl chains present in the dye resulted in a blue shift accompanied with a broadening of the absorption spectrum, for example, from **MK-1** to **MK-3** (Figure 2a) and from **MK-2** to **MK-4**, **MK-5**, and **MK-7** (Figure 2b). This indicates that the number of hexyl chains influences the intermolecular interaction. In addition, the broadness of the absorption spectrum for **MK-4**, **MK-5**, and **MK-7** is different, suggesting that the position

(41) Wang, Z.-S.; Kawauchi, H.; Kashima, T.; Arakawa, H. *Coord. Chem. Rev.* **2004**, *248*, 1381.
(42) Reichardt, C. *Chem. Rev.* **1994**, *94*, 2319.
(43) Socrates, G. *Infrared Characteristic Group Frequencies*, 2nd ed.; Willey & Sons Ltd: Baffins Lane, Chichester, U.K., 1994.
(44) Wang, Z.-S.; Sugihara, H. *Langmuir* **2006**, *22*, 9718.

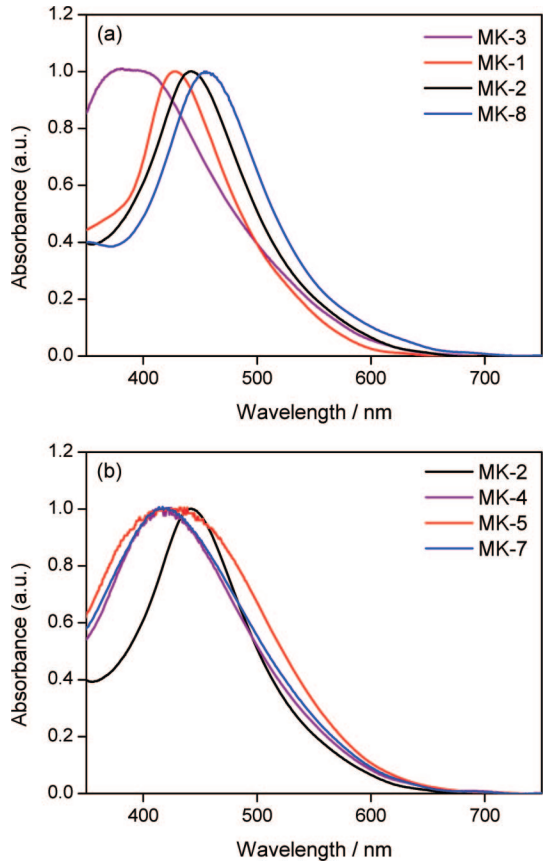

Figure 2. Normalized UV−vis absorption spectra for different **MK** dye-loaded TiO_2 films using a bare TiO_2 film as a reference. The transparent TiO_2 film (~1.5 μm) was dyed by dipping in 0.3 mM dye solution in toluene overnight.

of the hexyl chains also influences the intermolecular interaction. The blue spectral shift with reducing the number of hexyl chains suggests that **MK** dyes with less hexyl chains tend to form H-aggregates.[45] **MK-1**, **MK-2**, and **MK-8**, bearing one hexyl chain at each thiophene group, exhibit relatively sharp absorption peaks on the TiO_2 surface, suggesting their relatively weak intermolecular $\pi-\pi$ stacking as compared to the other **MK** dyes.

It is well-known that π-conjugated thiophene oligomers and polymers tend to π-stack due to the strong intermolecular interaction between π-electrons and between neighboring hydrophobic alkyl chains linked to the thiophene rings. The π-stacking structures for π-conjugated molecules such as oligothiophene have been investigated by NC-AFM, scanning tunneling microscopy (STM), and X-ray diffraction techniques.[46–50] For example, oligothiophenes, which have long alkyl chains such as dodecyl and hexyl, exhibit a lamella-type stacking of the oligothiophene backbone caused by an interlocking of the alkyl chains due to the interaction between alkyl chains.[46,49] On the contrary, the herringbone-type stacking was observed for a propyl- and nonsubstituted oligothiophene due to the decreased interaction between alkyl chains.[46,50] At present, we cannot determine the π-stacking structure of the **MK** dyes adsorbed on the TiO_2 surface because the **MK** dyes include the carbazole derivative and the cyanoacrylic acid, not just the oligothiophene backbone. However, the **MK** dyes probably adopt the similar molecular packing structures to those of the corresponding oligothiophenes,[46–50] which would depend on the position and number of the hexyl chains in the dye.

The strength of intermolecular interaction for the **MK** dyes with the same number of thiophenes, which may influence the solar-cell performance, can be compared by means of the adsorbed dye amount. We can see from Table 1 that the adsorbed amount of **MK-3** is larger than that of **MK-1** and that of **MK-2** is smaller than that of **MK-4**, **MK-5**, and **MK-7**. These data strongly support that the **MK** dyes with fewer hexyl chains have stronger intermolecular interaction than their counterparts with more hexyl chains on the TiO_2 surface. Note that not only the strong intermolecular interaction but also the small molecular size of **MK-3** is responsible for its large adsorbed amount. Intermolecular $\pi-\pi$ interaction, as compared to the interalkyl interaction, plays a key role in dye adsorption and more hexyl chains linked to the π-conjugated segment, which act as spacers, decrease intermolecular $\pi-\pi$ interaction, thus reducing the adsorbed dye amount. The difference of intermolecular $\pi-\pi$ interaction for **MK** dyes would account for their different broadness of UV−vis absorption spectra, as shown in Figure 2. We also observed that the adsorbed dye amount increased slightly with increasing the number of thiophene. This can be rationalized by the increased intermolecular $\pi-\pi$ interaction with expanding π-conjugation. Oligothiophene-based coumarin dyes follow the same tendency of the adsorbed dye amount as we reported previously,[51] further confirming that intermolecular $\pi-\pi$ interaction strengthens with increasing the number of thiophenes.

The formal oxidation potentials of the dyes adsorbed on the TiO_2 electrode were determined by CV. Taking the formal oxidation potential of the ground-state as HOMO and the absorption onset as the gap derived from Figure 2, the LUMO is estimated by their difference. The data for HOMO and LUMO are also listed in Table 1. All the LUMOs are more negative than the conduction band edge (−0.50 V vs NHE at pH = 1) of TiO_2 electrode,[36] which depends on the pH or composition of the electrolyte, ensuring that electron injection from the excited dye molecules into the conduction band of TiO_2 is thermodynamically favorable.

NC-AFM Measurement. NC-AFM images of the rutile TiO_2 (110) clean surface composed of curved steps and atomically flat terraces before and after adsorption of **MK-2** and a vertical profile along the line (a−b) are respectively

(45) Mooney, W. F.; Brown, P. E.; Russell, J. C.; Costa, S. B.; Pedersen, L. G.; Whitten, D. G. *J. Am. Chem. Soc.* **1984**, *106*, 5659.
(46) Azumi, R.; Götz, G.; Debaerdemaeker, T.; Bäuerle, P. *Chem. Eur. J.* **2000**, *6*, 735.
(47) Koren, A. B.; Curtis, M. D.; Francis, A. H.; Kampf, J. W. *J. Am. Chem. Soc.* **2003**, *125*, 5040.
(48) Curtis, M. D.; Cao, J.; Kampf, J. W. *J. Am. Chem. Soc.* **2004**, *126*, 4318.
(49) Kiriy, N.; Kiriy, A.; Bocharova, V.; Stamm, M.; Richter, S.; Plötner, M.; Fischer, W.-J.; Krebs, F. C.; Senkovska, I.; Adler, H.-J. *Chem. Mater.* **2004**, *16*, 4757.
(50) Barclay, T. M.; Cordes, A. W.; Mackinnon, C. D.; Oakley, R. T.; Reed, R. W. *Chem. Mater.* **1997**, *9*, 981.
(51) Hara, K.; Miyamoto, K.; Abe, Y.; Yanagida, M. *J. Phys. Chem. B* **2005**, *109*, 23776.

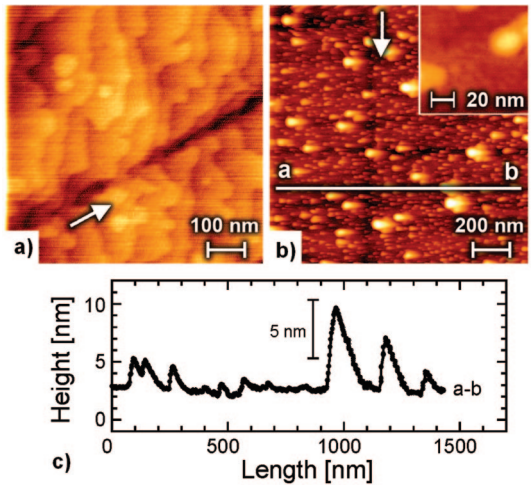

Figure 3. NC-AFM images of (a) the rutile TiO_2 (110) clean surface and of (b) the surface exposed to **MK-2** and a vertical profile (c) along the line (a, b). The inset shows a magnified area. Arrows indicate the substrate scratch line shown in a and b.

shown in Figure 3a−c. The terrace width is in the range of 10−100 nm, and the step height is about 0.3 nm, which corresponds to the single step height of the TiO_2 (110) surface. It is seen from Figure 3b,c that small particles whose diameter is about 10−100 nm and height is about 1 nm and large particles whose diameter is 40−100 nm and height is 2−10 nm were observed, which suggests that the surface was covered by two-dimensional (2D) and three-dimensional (3D) islands of dye aggregates. The formation of dye aggregates might originate from the strong intermolecular interaction.[46] It is worth noting that the substrate scratch line whose depth is on the order of nanometers is clearly observed in both AFM images, which is denoted by arrows, even on the **MK-2** adsorbed terrace. These observations suggest that the thickness of the **MK-2** monolayer may be equal to or thinner than the scratch depth.

Transient Absorption Spectroscopy. Figure 4a shows transient absorption monitored at 3440 nm for **MK-2**- and **MK-3**-loaded TiO_2 films after excitation at 540 nm, and Figure 4b depicts an energy diagram for a DSSC based on **MK-2**. In Figure 4a, the value of absorbance (0.015), which corresponds to 100% of electron injection yield, was estimated from the transient absorption data of a TiO_2 film sensitized by N3 dye, cis-bis(thiocyanato)bis(2,2′-bipyridyl-4,4′-dicarboxylic acid) ruthenium(II), whose electron injection yield from the excited dye to TiO_2 is 100%,[52] as a reference. In the transient absorption for **MK-3**-loaded TiO_2 film, the increasing absorption after photoexcitation of **MK-3** was observed, which is attributed to the injected electrons into the conduction band of TiO_2. The instantaneous rise of the transient absorption clearly indicates that electron injection from **MK-3** into the conduction band of TiO_2 occurred within 200 fs and the electron injection yield was almost unity.

On the other hand, more intense transient absorption for **MK-2** than that for **MK-3** was observed within 10 ps (Figure

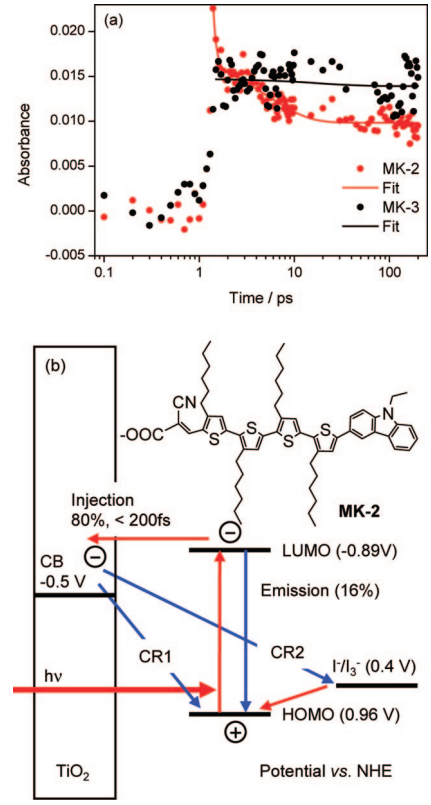

Figure 4. (a) Transient absorption monitored at 3440 nm for **MK-2** and **MK-3** adsorbed on a TiO_2 film after excitation at 540 nm and (b) schematic energy diagram for a DSSC based on **MK-2**, a nanocrystalline TiO_2 electrode, and the I^-/I_3^- redox couple.

4a) with decay times of 120 fs and 5 ps. The initial transient absorption for **MK-2**, which is higher than the unity value (0.015), includes the contribution from both the injected electrons and the intermolecular charge transfer species of oligothiophene. A similar transient absorption decay was observed for **MK-2**-loaded ZrO_2 film with a small contribution of long-lived species (<30%) as a reference, where electron injection cannot take place from **MK-2** because of the relatively negative conduction band edge level of ZrO_2 (data not shown). In addition, Ai et al. reported a similar transient absorption decay observed in SnO_2 and ZrO_2 nanocrystalline thin films sensitized by polythiophene derivatives within 10 ps, and they concluded that this transient absorption was due to quick generation of intermolecular charge-transfer species in the polythiophene moieties and the following relaxation processes, such as charge recombination and/or charge separation.[53] These results indicate that the transient absorption decay observed for **MK-2**-loaded TiO_2 film within 10 ps is attributed to the intermolecular charge-transfer species formed by **MK-2** dye molecules. Because this transient absorption due to intermolecular charge-transfer was not observed for **MK-3**, intermolecular interactions and thus the dye packing structure are clearly different between **MK-2** and **MK-3**.[53] The existence of long-lived transient absorption for **MK-2** indicates that ultrafast electron injection from **MK-2** to the conduction band of TiO_2 also takes place, as does **MK-3**.

(52) Katoh, R.; Furube, A.; Yoshihara, T.; Hara, K.; Fujihashi, G.; Takano, S.; Murata, S.; Arakawa, H.; Tachiya, M. *J. Phys. Chem. B* **2004**, *108*, 4818.

(53) Ai, X.; Anderson, N.; Guo, J.; Kowalik, J.; Tolbert, L. M.; Lian, T. *J. Phys. Chem. B* **2006**, *110*, 25496.

The electron injection efficiency was derived from the absolute absorbance at ~100 ps, where the absorbance due to intermolecular charge-transfer species of **MK-2** was almost negligible, using the electron injection yield for the N3 dye as a reference,[52] and the absolute magnitude of signals between different samples is reproducible (deviation within 10%). Although the random noise on these data is about 10%, the difference in absorbance between **MK-2** and **MK-3** after 10 ps is very evident (Figure 4a), indicative of different electron injection yields. The electron injection yield from **MK-2** to TiO_2 was thus estimated to be 70−90%, whereas that for **MK-3** was almost 100%.

NC-AFM data revealed that **MK-2** formed some 3D aggregates on the single crystal TiO_2 surface. It is well-known that the multilayer is less efficient for electron injection than the monolayer due to deactivation of the excited state via self-quenching processes arising from energy or charge transfer reactions between the 3D aggregated molecules.[54] In steady state emission measurement for a **MK-2**-loaded TiO_2 film, emission yield of 16% was observed. This value was estimated from a fluorescence intensity comparison between the **MK-2** sensitized TiO_2 film and the **MK-2** sensitized ZrO_2 film. Since the **MK-2** molecules forming the 3D aggregates undergo fluorescence quenching through intermolecular charge transfer to some extent, the quenching yield of 84% cannot exactly correspond to electron injection yield to TiO_2, giving some margin of error to this estimation. This, however, strongly supports that roughly 16% of **MK-2** molecules on the TiO_2 surface cannot inject electrons to TiO_2, explaining well the relatively lower electron injection yield (70−90%) for the **MK-2** dye-sensitized film. It is of note that the other **MK** dyes with hexyl chains also produced electron injection yield below unity, suggesting that the formed 3D aggregates should account for the lower electron injection yield. In contrast, **MK-3** is efficient for electron injection as evidenced by the electron injection yield of 100% and emission yield of 0%.

The dye adsorption is related to the molecular size and the thickness of dye aggregates as well. For molecules with similar size such as **MK-2**, **MK-4**, **MK-5**, and **MK-7**, a larger adsorbed amount would correspond to thicker aggregates, but for molecules with different size, we should consider the influence of molecular size on dye adsorption. On the basis of the data of injection and emission yields and its much smaller size as compared to **MK-1**, **MK-3** would form 2D dense packing rather than thick 3D aggregates.

Solar-Cell Performance. IPCE spectra for DSSCs based on one of the **MK** dyes as a function of wavelength are plotted in Figure 5. DSSCs based on dye-sensitized transparent TiO_2 (3.9 ± 0.1 μm) and electrolyte **A** were used for comparison of properties. DSSCs based on **MK-1**, **MK-2**, and **MK-3** produced maximum IPCE of ~75% while those based on the other dyes produced maximum IPCE below 70%. In particular, DSSCs based on **MK-4** and **MK-5** produced maximum IPCE below 60%. The maximum IPCE for DSSCs based on **MK-1** or **MK-2** did not reach the typical unity value (85−90%), taking 10−15% of absorption and

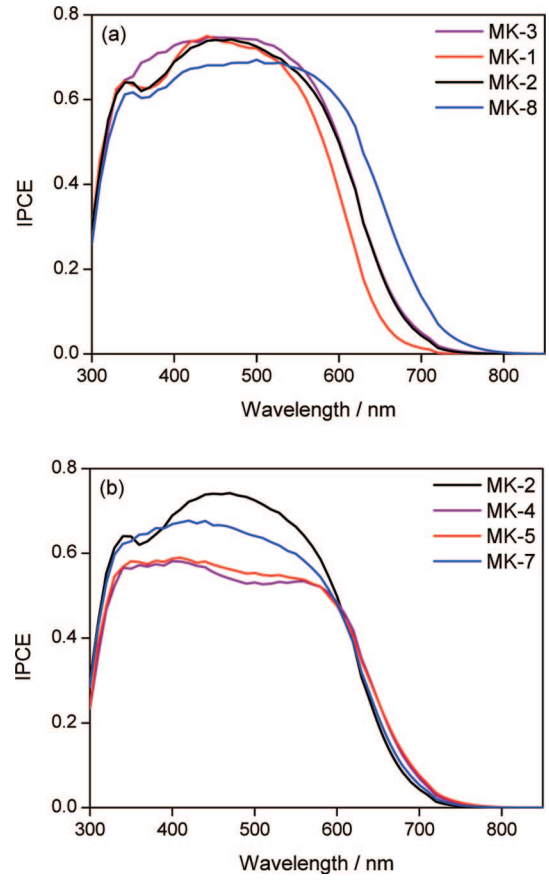

Figure 5. IPCE action spectra for DSSCs based on different **MK** dye-sensitized transparent TiO_2 films (3.9 ± 0.1 μm) with electrolyte **A**.

reflection by the substrate into account, because the electron injection yield was in the range of 70−90%. **MK-3** has electron injection yield of unity, but its maximum IPCE is around 75%, which is lower than expected. This is because the serious charge recombination in a DSSC based on **MK-3**, to be discussed later, reduces the photocurrent generation and hence the IPCE performance.

IPCE spectra gradually become broader toward the red region, from **MK-1** to **MK-2** and then to **MK-8** (Figure 5a) with increasing the number of thiophene units, consistent with the tendency of UV−vis absorption spectra of dye-loaded TiO_2 film (Figure 2a). Note that the low maximum IPCE for a DSSC based on **MK-8** is ascribed to its relatively low electron injection yield due to the low LUMO energy level (Table 1). For the **MK** dyes with quarter-thiophene, the reduction of hexyl chains lowers the maximum IPCE (Figure 5b).

The four dyes with quarter-thiophene showed almost same electron injection yield, but the dyes bearing two hexyl chains produced much lower maximum IPCE than **MK-2** with four hexyl chains (Figure 5b). IPCE is derived from the product of light harvesting efficiency (LHE) of the dye-loaded film, the quantum yield of the electron injection (CIE), and the efficiency of collecting the injected electron (CCE).[2] Since the absorbance is in the range of 1.8−3.4 for the dye-loaded ~1.5 μm TiO_2 film, the LHE should be very close to unity for all the dye-loaded TiO_2 films (3.8−4.0 μm). Electron injection yield is almost the same for the four dyes with quarter-thiophene, ruling out the possibility that the electron

(54) Khazraji, A. C.; Hotchandani, S.; Das, S.; Kamat, P. V. *J. Phys. Chem. B* **1999**, *103*, 4693.

Table 2. Solar-Cell Performance for DSSCs Based on an Individual MK Dye[a]

DSSC	J_{sc}, mA cm^{-2}	V_{oc}, V	FF	η (%)
MK-1	9.90	0.75	0.67	4.97
MK-2	10.67	0.69	0.68	5.01
MK-2[b]	10.93	0.73	0.68	5.43
MK-3	10.56	0.67	0.63	4.46
MK-4	5.72	0.74	0.48	2.03
MK-5	6.40	0.73	0.47	2.20
MK-5[c]	10.16	0.67	0.64	4.36
MK-7	10.41	0.74	0.46	3.54
MK-8	11.38	0.70	0.60	4.78

[a] Light source: 100 mW cm^{-2} AM1.5G simulated solar light. [b] $(C_2H_5)_3NH^+$ salt of **MK-2** was used. [c] Electrolyte **A** contained 0.2 M instead of 0.05 M iodine.

injection yield results in different IPCE. Therefore, CCE should account for the decreased maximum IPCE from a DSSC based on **MK-2** to DSSCs based on **MK-4**, **MK-5**, and **MK-7**. CCE is dependent on the charge transfer process of injected electrons across TiO_2 to the current collector, diffusion of I^- and I_3^- ions from and to the Pt counter electrode surface, reduction of I_3^- at the Pt/electrolyte interface, and regeneration of dye cations by I^- ions. Dye aggregates formed on the TiO_2 surface may block the diffusion of redox electrolyte through the nanoporous TiO_2 and then decreases the reduction rate of I_3^- at the Pt/electrolyte interface, to be discussed later, which would be the rate determining step for photocurrent generation. When the iodine content was increased from 0.05 to 0.2 M, increasing the concentration of I_3^- ions in the electrolyte, the IPCE at 480 nm for a DSSC based on **MK-5** increased dramatically from 56% to 70%. This suggests that the diffusion of I_3^- in the nanoporous TiO_2 electrode is blocked significantly by the dye layer, limiting the reduction of I_3^- at the Pt electrode and thus lowering the maximum IPCE to different extents depending on the adsorbed dye amount and/or dye aggregate thickness. The increasing content of I_3^- would accelerate reduction of I_3^- ions at the Pt electrode, giving improved IPCE.

The solar-cell performance for the DSSCs based on the **MK** dyes is summarized in Table 2. J_{sc} increased in the order of **MK-1** < **MK-2** < **MK-8** as a result of the broadening of IPCE action spectra with increasing the number of thiophene units. If the maximum IPCE of **MK-8**-based DSSC was comparable to that of **MK-2**-based DSSC, the J_{sc} of the former should be much higher. DSSCs based on **MK-4** and **MK-5** produced lower J_{sc} than a DSSC based on **MK-2**, as a result of lower IPCE of the former than that of the latter in the spectral range of 400−600 nm (Figure 5b).

A downward nonlinear relationship between current and light intensity was observed from about half-sun illumination for DSSCs based on **MK-4** and **MK-5** (Supporting Information), whereas a linear relationship was observed for DSSCs based on the other **MK** dyes, indicating that photocurrent generation is limited by the slow diffusion of I_3^- ions caused by the obstruction of dye aggregation. To compensate for the slow diffusion of I_3^- to the counter electrode, higher concentration of I_3^- is required to realize fast reduction of I_3^- at the counter electrode surface and thus efficient photocurrent generation. Consequently, when iodine content was increased from 0.05 to 0.2 M, a linear dependence of current on light intensity to one sun was recovered (Supporting Information). Electron injection yield might also be changed by adding iodine to the electrolyte, which would also influence photocurrent generation.

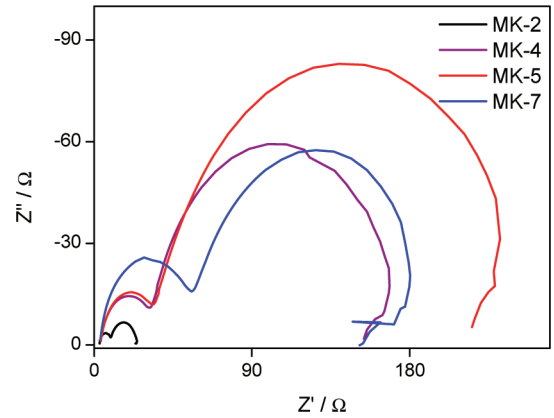

Figure 6. EIS Nyquist plots for DSSCs based on **MK-2**, **MK-4**, **MK-5**, and **MK-7** under one sun irradiation.

The hexyl chains affected the V_{oc} remarkably as reflected from the V_{oc} enhancement of ~80 mV from **MK-3** to **MK-1** (Table 2). In addition, DSSCs based on **MK-4**, **MK-5**, and **MK-7**, which showed larger adsorbed dye amount on the TiO_2 electrode, gave higher V_{oc} but lower FF as compared to a DSSC based on **MK-2**.

It was reported that the solar-cell performance can be modulated by adjusting the number of proton in N3.[55] A Ru dye with more protons can generate higher J_{sc} and lower V_{oc}, but the dye with less protons gives rise to a reverse result.[55] We also found that the photovoltaic performance depends on whether the proton is present in the **MK** dye. For example, when **MK-2** was changed from the acid to the $(C_2H_5)_3NH^+$ salt of **MK-2**, η was improved due to the significant increase in V_{oc}, as seen in Table 2.

Electrochemical Impedance Spectroscopy. The above-mentioned changing tendencies of FF and V_{oc} can be clarified by EIS, which is a powerful technique of characterizing the important interfacial charge transfer processes in a DSSC. Figure 6 shows the EIS Nyquist plot for DSSCs based on **MK-2**, **MK-4**, **MK-5**, and **MK-7**. The small and large semicircles respectively located in the high- and middle-frequency regions, are assigned to the charge transfer at Pt/electrolyte and TiO_2/dye/electrolyte interface, respectively.[56,57] Another small semicircle, which should have appeared at the low-frequency region, is overlapped by the middle-frequency large semicircle. The charge transfer resistance (R_{CT}) at the Pt/electrolyte interface, which inversely scales with the reduction rate of I_3^- ions at the Pt/electrolyte interface, is estimated by the small semicircle width. A small R_{CT} means fast reduction of I_3^- ions at Pt or fast diffusion of I_3^- ions through nanoporous TiO_2 to the Pt counterelectrode and vice versa. One can see from Figure 6 that R_{CT} for a DSSC with **MK-2** is much smaller than those for

(55) Nazeeruddin, M. K.; Humphry-Baker, R.; Liska, P.; Grätzel, M. *J. Phys. Chem. B* **2003**, *107*, 8981.
(56) Longo, C.; Nogueira, A. F.; De Paoli, M.-A.; Cachet, H. *J. Phys. Chem. B* **2002**, *106*, 5925.
(57) Kern, R.; Sastrawan, R.; Ferber, J.; Stangl, R.; Luther, J. *Electrochim. Acta* **2002**, *47*, 4213.

Scheme 1. Schematic Representation of CR2 (Brown Arrow), Diffusion of I_3^- Ions in Nanoporous TiO_2 (Blue Arrow), and Reduction of I_3^- Ions at the Pt/Electrolyte Interface (Orange Arrow) for DSSCs Consisting of (a) Thin and (b) Thick Dye Layers on the TiO_2 Surface

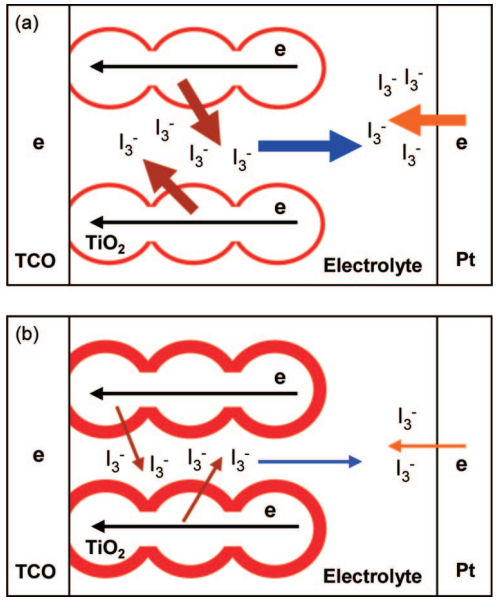

DSSCs with **MK-4**, **MK-5**, and **MK-7**, indicating that the diffusion of I_3^- ions through nanoporous TiO_2 in the former DSSC is more smooth than that in the latter three DSSCs. Why is the diffusion for DSSCs with **MK-4**, **MK-5**, and **MK-7** much slower than that for a DSSC with **MK-2**? We suppose that the diffusion of I_3^- ions, generated during the oxidation of I^- ions by the oxidized dye, to the Pt surface is blocked by the dye layer in the nanoporous TiO_2 electrode, as illustrated in Scheme 1. **MK-4**, **MK-5**, and **MK-7** would form a thicker aggregate layer than **MK-2** on the TiO_2 surface since the adsorbed dye amount of the former is much larger than that of the latter (Table 1), and it is reasonable that a thicker dye layer leads to slower diffusion of redox species in the nanoporous TiO_2 electrode. When iodine content was increased from 0.05 to 0.2 M, increasing content of I_3^- ions, more I_3^- ions are present near the Pt counter-electrode, and we simultaneously observed decreased R_{CT} and increased FF, strongly supporting that the slow diffusion, caused by the blocking effect of dye aggregate, is responsible for the lower FF.

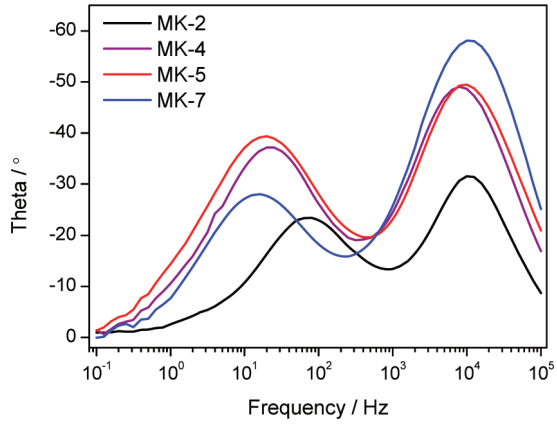

Figure 7. EIS Bode plots for DSSCs based on **MK-2**, **MK-4**, **MK-5**, and **MK-7** under one sun irradiation.

On the contrary, DSSCs based on **MK-4**, **MK-5**, and **MK-7** produced higher V_{oc} than a DSSC based on **MK-2**, which can be explained by the electron lifetime. Figure 7 shows the Bode plot for DSSCs based on **MK-2**, **MK-4**, **MK-5**, and **MK-7**. Two peaks in Figure 7 located at high frequency (right) and middle frequency (left) respectively correspond to the small semicircle (left) and large semicircle (right) in the Nyquist plot (Figure 6). The reciprocal of the peak frequency for the middle-frequency peak is regarded as the electron lifetime since it represents the charge transfer process at the TiO_2/dye/electrolyte interface. It is evident that the electron lifetime for the DSSC based on **MK-2** is smaller than that for DSSCs based on **MK-4**, **MK-5**, and **MK-7**, thereby explaining the V_{oc} increase from **MK-2** to **MK-4**, **MK-5**, and **MK-7**. Consistent with this result, the charge transfer (i.e., CR2) resistance at the TiO_2/dye/electrolyte interface increased from **MK-2** to **MK-4**, **MK-5**, and **MK-7** as seen in Figure 6. As we previously mentioned, **MK-4**, **MK-5**, and **MK-7** showed larger adsorbed dye amount and/or thicker dye aggregate on the TiO_2 surface compared to **MK-2** due to the stronger intermolecular $\pi-\pi$ interaction. Since the dye layer on the TiO_2 surface acts as a blocking layer preventing CR2,[58] and **MK-4**, **MK-5**, and **MK-7** would block the approach of I_3^- ions to the TiO_2 surface for CR2 more efficiently than **MK-2**, as demonstrated in Scheme 1. For this reason, the DSSCs based on **MK-4**, **MK-5**, and **MK-7** have longer electron lifetime than a DSSC with **MK-2**. With respect of the prevention of electron leakage to redox electrolyte, the dye packing layer has the similar function to the thin insulating layer coated on the TiO_2 surface as reported in the literature.[59,60]

Finally the remarkable effect of hexyl chains on V_{oc} is also interpreted by the electron lifetime. Figure 8a depicts the Bode plot for DSSCs based on **MK-1** and **MK-3**, where the middle-frequency peak shifted to a smaller frequency from **MK-3** to **MK-1** under one sun irradiation, indicating that electron lifetime was improved by the hexyl chains, consistent with our previous result measured by the transient photovoltage technique.[38] The dependence of electron lifetime on J_{sc}, which was measured at the same light intensity for EIS measurement and almost equals injected current density because charge recombination at short circuit is negligible, is shown in Figure 8b. For both DSSCs, electron lifetime decreases with increasing J_{sc} following a power-law relation. The electron lifetime for a DSSC based on **MK-1** is ~9 times as large as that for a DSSC based on **MK-3** at the same J_{sc}, accounting for the remarkable increase in V_{oc} from **MK-3** to **MK-1**.

Several groups have investigated the alkyl chain effect on charge recombination and photovoltaic performance. In the case of Ru dyes, Kroeze et al. concluded that the alkyl chain

(58) Ito, S.; Liska, P.; Comte, P.; Charvet, R.; Péchy, P.; Bach, U.; Schmidt-Mende, L.; Zakeeruddin, S. M.; Kay, A.; Nazeeruddin, M. K.; Grätzel, M. *Chem. Commun.* **2005**, 4351.
(59) Palomares, E.; Clifford, J. N.; Haque, S. A.; Lutz, T.; Durrant, J. R. *J. Am. Chem. Soc.* **2003**, *125*, 475.
(60) Wang, Z.-S.; Yanagida, M.; Sayama, K.; Sugihara, H. *Chem. Mater.* **2006**, *18*, 2912.

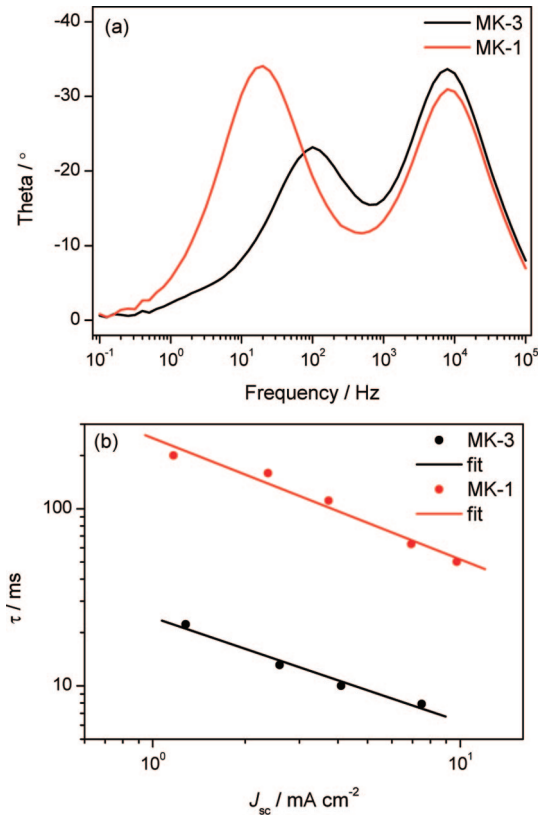

Figure 8. (a) Bode plot under irradiation of one sun and (b) electron lifetime against J_{sc}, which was measured at the same light intensity for EIS measurement, for DSSCs based on **MK-3** and **MK-1**.

itself is effective to slow charge recombination,[61] whereas Mori et al. reported that the alkyl chain itself does not impede the approach of I_3^- ions to the TiO_2 surface,[62] indicating that the alkyl chain effect is still controversial. Matsui et al. reported that the V_{oc} for DSSCs based on squaraine dyes was improved with increasing the alkyl chain length.[63] For **MK** dyes, we simultaneously observed enhanced electron lifetime and V_{oc} by the hexyl chains. One possibility is the blocking effect of the hexyl chain itself. The hydrophobic hexyl chains act as barriers preventing hydrophilic I_3^- ions approaching the TiO_2 surface, thereby retarding CR2. Another possibility comes from the effect of dye aggregate on charge recombination. The thick 3D aggregates of **MK-1** would be more effective than the thin 2D packing of **MK-3** to suppress CR2 (Scheme 1). We cannot conclude that the increased electron lifetime from **MK-3** to **MK-1** is intrinsically due to the alkyl chains, the formed thicker aggregates in **MK-1**, or both. The two kinds of effects would be distinguished if the aggregates of **MK-1** and **MK-3** would be tuned in light of man's need.

Best Solar-Cell Performance. MK-2 is best among the series of **MK** dyes in terms of efficiency (Table 2). We therefore focused on the optimization of DSSCs with **MK-2** based on the above fundamental findings. A DSSC consisting

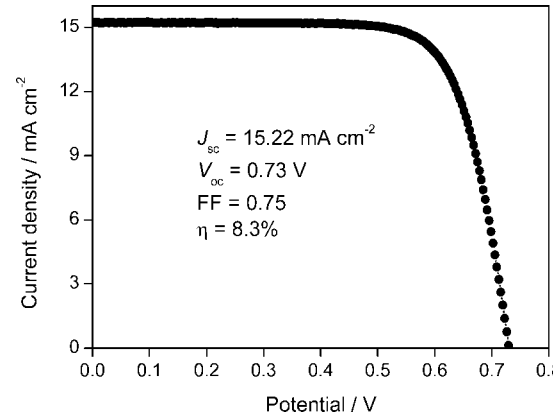

Figure 9. $I-V$ curve for a DSSC based on $(C_2H_5)_3NH^+$ salt of **MK-2** under illumination of 100 mW cm^{-2} AM1.5G simulated light. Electrolyte **C** was used. An aperture mask (0.2354 cm^2) was put on the cell surface to avoid the diffuse light.

of an **MK-2** sensitized TiO_2 electrode (16 μm), as detailed in the Experimental Section, produced η of 7.6% (J_{sc} = 14.20 mA cm^{-2}, V_{oc} = 0.74 V, FF = 0.72) with electrolyte **B**. The η dramatically went up to 8.3% (J_{sc} = 15.22 mA cm^{-2}, V_{oc} = 0.73 V, FF = 0.75) when electrolyte **C** was used, as shown in Figure 9. The improvements of J_{sc} and FF, attributable to the enhanced electrolyte diffusion with increasing the iodine concentration,[64] suggest that a smaller amount of adsorbed **MK-2**, as compared to **MK-5**, also blocks diffusion of electrolyte. Note that a DSSC based on N719 produced η of 8.9% with electrolyte **B** but of 8.1% with electrolyte **C** since the significantly decreased J_{sc} and V_{oc} offset the slightly increased FF with increasing iodine content. These data clearly indicate that the **MK** dyes with hexyl chains are favorable for suppressing CR2, especially at high content of I_3^- ions, due to the presence of hexyl chains and the thick aggregate they formed on the TiO_2 surface, as compared to N719. The 8.3% of η for the DSSC based on **MK-2** is among the highest values[10,32,65] obtained from DSSCs based on metal-free organic dyes and is close to that for the DSSC based on N719 dye under each optimal condition, indicative of successful molecular design toward high V_{oc} and η. If the photoresponse can be extended to longer wavelength, similar or higher η would be expected.

Conclusions

We designed and synthesized a series of novel carbazole dyes (**MK** dyes), which have different hexyl substituted thiophene moieties as a π-conjugation system, for application in DSSCs. The modification of the **MK** dyes in terms of the number and position of hexyl chains is an effective method to control adsorbed dye amount and/or dye aggregate thickness on the TiO_2 surface, which determines the charge recombination and solar-cell performance. A DSSC based on **MK-2** consisting of four hexyl-substituted thiophenes produced 8.3% of η, which is comparable to 8.1% for the DSSC based on N719 under a comparable condition.

(61) Kroeze, J. E.; Hirata, N.; Koops, S.; Nazeerruddin, Md., K.; Schmidt-Mende, L.; Grätzel, M.; Durrant, J. R. *J. Am. Chem. Soc.* **2006**, *128*, 16376.
(62) Mori, S. N.; Kubo, W.; Kanzaki, T.; Masaki, N.; Wada, Y.; Yanagida, S. *J. Phys. Chem. C* **2007**, *111*, 3522.
(63) Matsui, M.; Nagasaka, K.; Tokunaga, S.; Funabiki, K.; Yoshida, T.; Minoura, H. *Dyes Pigm.* **2003**, *58*, 219.
(64) Liang, L.; Dai, S.; Hu, L.; Kong, F.; Xu, W.; Wang, K. *J. Phys. Chem. B* **2006**, *110*, 12404.
(65) Ito, S.; Zakeeruddin, S. M.; Humphry-Baker, R.; Liska, P.; Charvet, R.; Comte, P.; Nazeeruddin, M. K.; Péchy, P.; Takata, M.; Miura, H.; Uchida, S.; Grätzel, M. *Adv. Mater.* **2006**, *18*, 1202.

In addition to the alkyl chain effect on electron lifetime and V_{oc} as we reported in the previous communication,[38] we found that CR2 and the diffusion of electrolyte through the nanoporous TiO_2 electrode depend on the amount and/or aggregate thickness of adsorbed dyes, the latter being tunable by the molecular structure in terms of alkyl chain number and position. For the **MK** dyes with alkyl chains, electron lifetime, and V_{oc} increased with increasing the amount and/or aggregate thickness of adsorbed dyes. On the contrary, large amount and/or thick aggregate of adsorbed dyes decreased FF and J_{sc} significantly because the dye layer suppresses diffusion of redox species through the nanoporous TiO_2 electrode. Such a dilemma could be overcome by increasing iodine content in the redox electrolyte, resulting in improved J_{sc} and FF with comparable V_{oc}.

AFM data, however, reveals that some 3D aggregates of **MK-2** were formed on the TiO_2 surface, thereby reducing electron injection yield and hence photocurrent. To obtain better solar-cell performance, further molecular design taking into consideration the above results is necessary.

Acknowledgment. This work was supported by Industrial Technology Research Grant Program in '05 from New Energy and Industrial Technology Development Organization (NEDO) of Japan. We also thank Dr. Reiko Azumi for useful discussion about intermolecular interaction in substituted oligothiohenes.

Supporting Information Available: Synthesis procedures, characterization of all compounds, FT-IR data, and relationship between J_{sc} and light intensity for a DSSC based on **MK-5**. This material is available free of charge via the Internet at http://pubs.acs.org.

CM8003276